ACCSCIENCE PUBLISHING

Materials Science in Additive Manufacturing

ORIGINAL RESEARCH ARTICLE

Processing–structure–property correlation in AA2024-reinforced PETG composites fabricated via FDM: Experimental characterization and hybrid AHP–TOPSIS optimization

Raja Subramani[1], Rajeswari Nageswaran[2], Jaiprakash Narain Dwivedi[3], Mohamad Reda A. Refaai[4]*, Saad Rashed Alquraini[5], Mukhtar Fatihu Hamza[6], and Babatunde Omoniyi Odedairo[7]

[1]Department of Mechanical Engineering, Saveetha Engineering College, Chennai, Tamil Nadu, India

[2]Department of Mechanical Engineering, Chennai Institute of Technology, Chennai, Tamil Nadu, India

[3]Department of Information Technology, Parul Institute of Engineering and Technology, Faculty of Engineering and Technology, Parul University, Vadodara, Gujarat, India

[4]Department of Mechanical Engineering, College of Engineering in Al-Kharj, Prince Sattam bin Abdulaziz University, Al-Kharj, Riyadh Province, Saudi Arabia

[5]Department of Industrial Engineering, College of Engineering in Al-Kharj, Prince Sattam bin Abdulaziz University, Al-Kharj, Riyadh Province, Saudi Arabia

[6]Department of Mechatronics Engineering, Faculty of Engineering, Bayero University, Kano, Kano State, Nigeria

[7]Department of Industrial and Production Engineering, Faculty of Technology, University of Ibadan, Ibadan, Oyo State, Nigeria

***Corresponding author:** Mohamad Reda A. Refaai (m.rifaee@psau.edu.sa)

Citation: Subramani R, Nageswaran R, Dwivedi JN, *et al*. Processing–structure–property correlation in AA2024-reinforced PETG composites fabricated via FDM: Experimental characterization and hybrid AHP–TOPSIS optimization. *Mater Sci Add Manuf*. 2026;5(3):026210045. doi: 10.36922/MSAM026210045

Received: April 19, 2026

Revised: May 21, 2026

Accepted: June 2, 2026

Published online: July 3, 2026

Abstract

Metallic-reinforced thermoplastic composites fabricated via fused deposition modeling (FDM) offer a sustainable and material-efficient pathway for achieving enhanced functional performance; however, challenges related to uniform particle dispersion and interfacial bonding remain critical. In this study, the processing–structure–property correlation of AA2024 metal powder-reinforced polyethylene terephthalate glycol (PETG) composites was systematically investigated. Composite filaments containing 0–7.5 wt.% AA2024 were fabricated and processed under varying parameters, including layer height, infill density, and nozzle temperature. The resulting mechanical properties—tensile, flexural, and compressive strengths—along with wear behavior were evaluated, supported by microstructural characterization using scanning electron microscopy and energy-dispersive spectroscopy. The results revealed that an optimal reinforcement content of 5 wt.% AA2024 led to improvements of 19.8%, 17.6%, and 20.2% in tensile, flexural, and compressive strengths, respectively, accompanied by a significant reduction in wear rate of 40.5%. The enhanced performance is attributed to improved load transfer and microstructural integrity at optimal dispersion levels. Furthermore, a hybrid multi-criteria decision-making framework based on the analytical hierarchy process–technique for order preference by similarity to ideal solution (AHP–TOPSIS) was employed to identify the optimal processing conditions. The developed composite system demonstrates potential for efficient material utilization and advanced additive manufacturing applications, which are consistent with sustainable development goals.

Keywords: Fused deposition modeling; Polyethylene terephthalate glycol composites; AA2024 reinforcement; Sustainable Development Goals; Processing–structure–property relationship; Sustainable additive manufacturing materials; Analytical hierarchy process–technique for order preference by similarity to ideal solution (AHP–TOPSIS) optimization

1. Introduction

Additive manufacturing has emerged as one of the most transformative manufacturing technologies because of its capability to fabricate complex geometries directly from computer-aided design (CAD) models, with minimal material wastage and reduced tooling requirements. Unlike conventional subtractive manufacturing processes, additive manufacturing constructs components layer by layer, offering exceptional design flexibility, shortened production cycles, and enhanced customization potential. Among various additive manufacturing technologies, fused deposition modeling (FDM) has gained widespread industrial and academic acceptance due to its cost-effectiveness, ease of operation, material availability, and adaptability for both rapid prototyping and functional engineering applications. FDM technology operates by extruding thermoplastic materials through a heated nozzle in a layer-wise manner to create 3D structures with controlled geometrical features. Owing to its simplicity and scalability, FDM has been extensively utilized in automotive, aerospace, biomedical, and consumer product applications.[1] However, despite its numerous advantages, conventionally printed FDM parts frequently exhibit several limitations, including low mechanical strength, anisotropic behavior, inadequate wear resistance, poor thermal stability, and insufficient interlayer bonding. These limitations restrict the direct use of pure thermoplastic materials in demanding structural and tribological applications where superior load-bearing capability and dimensional stability are required.

To overcome these shortcomings, significant research attention has been directed toward the development of reinforced polymer composites suitable for FDM processing. The incorporation of ceramic, carbon-based, and metallic fillers into thermoplastic matrices has demonstrated considerable potential for improving mechanical, thermal, and tribological performance. In particular, metal-reinforced polymer composites have attracted increasing interest because metallic fillers can enhance stiffness, hardness, thermal conductivity, and wear resistance of printed structures. Several studies have demonstrated that the addition of metallic reinforcements can improve stress-transfer capability and modify the fracture characteristics of polymer matrices under loading conditions.[2,3] Nevertheless, achieving uniform filler dispersion, stable extrusion behavior, and strong particle–matrix interaction remains a significant challenge during filament fabrication and FDM processing. Excessive filler concentration often results in particle agglomeration, increased melt viscosity, nozzle clogging, and poor interlayer adhesion, ultimately deteriorating the final properties of printed components.

Among commercially available thermoplastics, polyethylene terephthalate glycol (PETG) has emerged as a promising material for FDM applications due to its balanced combination of mechanical strength, ductility, chemical resistance, dimensional stability, and excellent printability. Compared with commonly used polymers, such as polylactic acid (PLA) and acrylonitrile butadiene styrene (ABS), PETG exhibits improved impact resistance, enhanced interlayer bonding, lower shrinkage tendency, and reduced warpage during printing. These characteristics make PETG particularly attractive for engineering applications requiring reliable structural integrity and processing stability. Several recent investigations have highlighted the suitability of PETG for the fabrication of reinforced composites using FDM technology. For example, Mahesh *et al.*[4] reported that PETG-based composites demonstrated improved dimensional accuracy and reduced printing defects compared with conventional PLA composites. Similarly, Loknath and Vakkalagadda[5] observed enhanced impact performance and superior layer adhesion in PETG composites reinforced with particulate fillers. Samaan *et al.*[6] further demonstrated that optimized PETG composites exhibited favorable tensile and flexural properties due to improved compatibility between the matrix and reinforcement phases. Although PETG has shown considerable promise as a matrix material, studies involving PETG reinforced with metallic particles remain limited when compared with PLA-based composite systems.

Aluminum alloy reinforcements, particularly AA2024, have attracted substantial interest due to their excellent strength-to-weight ratio, fatigue resistance, corrosion resistance, and favorable tribological characteristics. AA2024 contains copper, magnesium, and manganese as major alloying elements, which contribute significantly to its mechanical performance and wear resistance.

The incorporation of AA2024 particles into polymer matrices may therefore provide a viable pathway for improving the structural and tribological behavior of FDM-fabricated composites. Demir *et al.*[7] investigated aluminum-filled thermoplastic composites and reported notable improvements in tensile stiffness and hardness up to an optimal filler concentration, beyond which particle agglomeration negatively affected performance. Vinay *et al.*[8] analyzed the flexural response of metal-filled polymer composites and emphasized the importance of filler dispersion and interfacial interaction in determining load-bearing capability. Vardhan *et al.*[9] examined aluminum–PLA composites fabricated through FDM and observed enhanced tensile strength and elastic modulus due to the rigid metallic reinforcement, although ductility decreased at higher reinforcement contents. James *et al.*[10] studied the tribological performance of metallic-particle-reinforced polymer composites and reported reduced wear rates under optimized reinforcement conditions. Similarly, Tanveer *et al.*[11] investigated the influence of FDM processing parameters on the mechanical behavior of reinforced thermoplastic composites and highlighted the critical role of layer height, raster orientation, and infill density. Akhoundi *et al.*[12] demonstrated that nozzle temperature and print speed strongly influence interlayer bonding and dimensional accuracy of FDM-printed composite specimens, while Omer *et al.*[13] reported that optimized printing conditions significantly improved wear resistance and compressive strength.

In addition to material development, process-parameter optimization has become an essential aspect of additive manufacturing research because multiple interacting variables influence the final properties of printed parts. Parameters such as nozzle temperature, layer height, infill density, raster angle, print speed, and build orientation can significantly affect interlayer bonding, porosity formation, residual stresses, and mechanical performance. Conventional single-response optimization techniques are often inadequate for evaluating additive manufacturing systems because improvements in one property may adversely affect another. Consequently, multi-criteria decision-making (MCDM) approaches have gained increasing importance for optimizing complex FDM processes involving conflicting performance requirements. Among these methods, the analytical hierarchy process (AHP) and technique for order preference by similarity to ideal solution (TOPSIS) have demonstrated strong capability for systematic decision-making and parameter ranking. AHP enables assignment of relative importance weights to performance criteria through pairwise comparison analysis, while TOPSIS ranks experimental alternatives according to their distances from the ideal and negative-ideal solutions. Recent studies by Singh *et al.*,[14] Kitila *et al.*,[15] and Al-Ibadi *et al.*[16] successfully applied hybrid AHP–TOPSIS frameworks for the optimization of additive manufacturing processes involving multiple performance criteria, such as tensile strength, surface quality, dimensional accuracy, and wear resistance.

Despite these advancements, several important research gaps remain unresolved in the existing literature. Most studies involving metal-filled FDM composites have focused primarily on PLA- or ABS-based systems, while comparatively limited attention has been devoted to PETG reinforced with aluminum-alloy particles such as AA2024. Furthermore, many previous investigations have concentrated either on mechanical characterization or process optimization independently, without establishing a comprehensive processing–structure–property relationship for reinforced PETG composites. Limited studies have systematically evaluated the combined influence of reinforcement concentration and FDM process parameters on tensile, flexural, compressive, and tribological performance simultaneously. In addition, there remains insufficient understanding regarding the optimal reinforcement concentration capable of balancing mechanical enhancement, printability, dimensional stability, and wear resistance in AA2024-reinforced PETG systems.

Therefore, the present work aims to investigate the processing–structure–property relationships of AA2024-reinforced PETG composites fabricated through FDM technology. The effects of reinforcement concentration and selected FDM processing parameters on the mechanical and tribological behavior of the fabricated composites were systematically evaluated. Furthermore, a hybrid AHP–TOPSIS optimization framework was implemented to identify the optimal parameter combination capable of achieving balanced overall performance. The study is expected to contribute toward the development of advanced metal-reinforced PETG composites for engineering applications requiring enhanced mechanical reliability and tribological stability.

Several researchers have also emphasized the significance of filament preparation parameters in determining the printability and final performance of FDM-fabricated composites. Parameters such as extrusion temperature, screw speed, cooling rate, filament diameter consistency, and moisture control strongly influence particle dispersion, interfacial bonding, and porosity formation within composite filaments. Improper filament fabrication conditions often result in nozzle clogging, dimensional instability, and poor interlayer adhesion during printing. In addition, optimization of FDM processing parameters, including layer height, raster angle, nozzle temperature, printing speed, and infill density, has been widely investigated using statistical and multi-criteria optimization approaches, such as Taguchi design, response surface methodology, gray relational analysis, AHP, and TOPSIS. These studies demonstrated that parameter optimization plays a critical role in balancing mechanical strength, dimensional accuracy, surface quality, and tribological performance in additively manufactured polymer composites. However, several important research gaps still exist in the current literature. Most existing studies on metal-filled FDM composites have primarily focused on PLA- or ABS-based systems, while comparatively limited attention has been given to PETG-based composites reinforced with aluminum alloys such as AA2024. PETG possesses distinct advantages, including improved ductility, enhanced interlayer adhesion, and superior chemical resistance, compared with commonly used thermoplastics, yet the processing–structure–property relationships in PETG/metal composite systems remain insufficiently understood. In particular, only a limited number of studies have investigated how AA2024 particle dispersion, interfacial bonding quality, and FDM processing parameters collectively influence the mechanical and tribological behavior of PETG composites.

Furthermore, many previous investigations have evaluated mechanical properties or process parameters independently without establishing a comprehensive correlation between material formulation, microstructural evolution, and final performance characteristics. The combined influence of reinforcement concentration and FDM process settings on tensile, flexural, compressive, and wear properties has not been systematically investigated for AA2024-reinforced PETG composites. Additionally, although optimization techniques have frequently been used in additive manufacturing studies, most approaches focus on single-response optimization and often fail to simultaneously account for multiple conflicting performance criteria relevant to practical engineering applications.

The need for conducting the current research stems from the growing demand for materials with high strength, low weight, and wear resistance that can be produced using affordable additive manufacturing methods. It is feasible to create composite materials with improved mechanical and tribological properties by combining the benefits of AA2024 aluminum alloy with the good processability of PETG. Nevertheless, the successful development of materials of interest requires understanding how different processing conditions affect microstructural characteristics and, in turn, composite properties. Consequently, the key goal of this work is to produce and examine AA2024-reinforced PETG composites via FDM and to reveal the relationships among processing, microstructure, and properties. Composite filaments were prepared with varying weight fractions of AA2024 alloy and evaluated experimentally for their tensile, flexural, compressive, and wear behavior. Furthermore, SEM and EDS were used to analyze the microstructure and elemental composition.

The selection of the hybrid AHP–TOPSIS optimization framework in the present study was motivated by the multi-response nature of FDM composite performance evaluation. Unlike single-objective optimization methods that focus on only one parameter at a time, the hybrid AHP–TOPSIS approach enables simultaneous consideration of multiple conflicting criteria such as tensile strength, flexural strength, compressive strength, wear resistance, printability, and dimensional accuracy. The AHP method provides a systematic mechanism for assigning relative importance to engineering performance criteria based on expert judgment, while TOPSIS enables ranking alternatives based on their closeness to an ideal solution. Compared with conventional optimization techniques, such as single-response Taguchi analysis or basic regression-based approaches, the hybrid AHP–TOPSIS framework offers improved decision-making capability for complex additive manufacturing systems involving multiple interacting process variables and performance objectives. One of the novel aspects of this research is the coupling of experimental analysis with a hybrid MCDM approach using AHP and TOPSIS to determine the optimal material formulation and FDM process parameter settings. Contrasting with the usual approach of focusing on only one property or variable at a time, this proposed model can evaluate multiple performance characteristics simultaneously, enabling a more holistic approach to solving the problem. Additionally, by establishing a connection between various microstructural features, such as the degree of dispersion or agglomeration of the reinforcing particles, and the resulting material performance, a better understanding of the physical basis of composite behavior can be gained. The determination of the optimal level of reinforcement, together with the ideal process conditions, can lead to improved materials and valuable insights into metal-polymer composites production.

The rest of the paper is arranged in the following manner: Section 2 discusses material selection, the composite production procedure, FDM process parameters, the experimental methodology, and the hybrid AHP–TOPSIS optimization approach. Section 3 illustrates the findings and discussion regarding the mechanical characteristics, wear characteristics, microstructural evaluation, and optimization analysis, with particular emphasis on the relationships between the process, microstructure, and properties. The concluding remarks of the paper are presented in Section 4.

2. Materials and methods

2.1. Materials

The matrix material selected for the present study was PETG filament (eSUN Industrial Co., Ltd., China), an amorphous glycol-modified thermoplastic polyester widely used in FDM due to its excellent printability, low shrinkage behavior, and improved interlayer adhesion compared with conventional thermoplastics such as PLA and ABS. The PETG filament possessed a nominal diameter of 1.75 mm, a density of 1.27 g/cm^3, a glass transition temperature in the range of 75–85 °C, and suitable melt-flow characteristics for stable FDM processing.

The reinforcement material selected in this work was AA2024 aluminum alloy powder procured from Vedayukt India Private Limited, Jharkhand, India. The reinforcement was selected for its high strength-to-weight ratio, enhanced fatigue resistance, and improved wear resistance, all of which are associated with its copper-rich alloy composition. The selected AA2024 powder possessed a purity greater than 99 wt.% with particle sizes ranging from 10 μm to 50 μm and irregular semi-spherical morphology. The alloy composition primarily consisted of aluminum with copper (4.4 wt.%), magnesium (1.5 wt.%), and manganese (0.6 wt.%) as the major alloying elements.

Prior to composite fabrication, the AA2024 powder was dried at 80 °C for 4 h to remove absorbed moisture and minimize porosity formation during melt processing. Similarly, the PETG filament was maintained under controlled humidity conditions to reduce hydrolytic degradation during filament preparation and FDM printing. The overall experimental workflow, including composite preparation, FDM fabrication, and tribological characterization, is illustrated in Figure 1.

2.2. Composite preparation

The manufacturing process of AA2024-reinforced PETG composites consisted of three distinct stages: dry blending, melt compounding, and filament extrusion. To start, predetermined mass fractions (0 wt.%, 2.5 wt.%, 5 wt.%, and 7.5 wt.%) of AA2024 powders were weighed using an electronic scale, ensuring ±0.001 g precision in mass measurements. The PETG pellets, produced by mechanical cutting of commercially available filament, were mixed with AA2024 powders using a Turbula® T2F three-dimensional shaker mixer (Willy A. Bachofen AG, Switzerland) to obtain initial homogeneity. The mixing process was conducted at 49 rpm for 30 min under ambient laboratory conditions. The three-dimensional motion of the mixer facilitated uniform dispersion of AA2024 particles within the PETG feedstock prior to melt compounding.

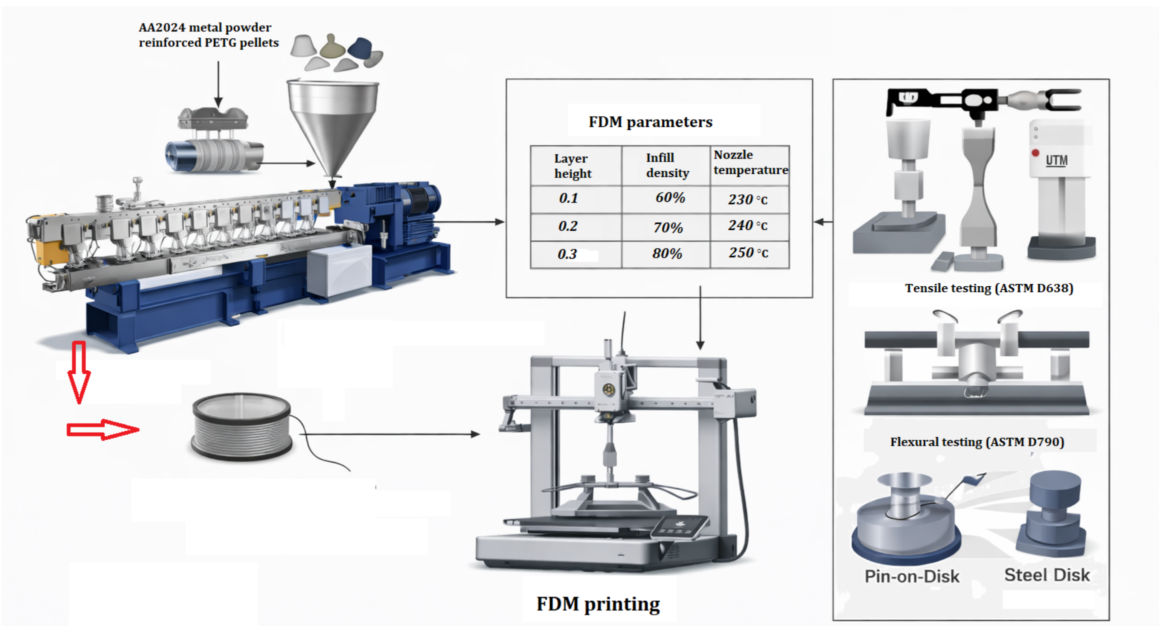

Figure 1. Schematic illustration of the experimental setting for the fabrication and characterization of AA2024-reinforced polyethylene terephthalate glycol (PETG) composites, including composite filament extrusion, fused deposition modeling (FDM)-based specimen fabrication, and subsequent mechanical (tensile—ASTM D638, flexural—ASTM D790, compression—ASTM D695) and tribological (pin-on-disk) testing procedures

In the second stage, the blend was melt-compounded using a laboratory-scale single-screw filament extruder (Noztek Pro Filament Extruder, Noztek Ltd., United Kingdom) with a temperature-regulated barrel. During filament fabrication, the extrusion temperature was maintained at 230–245 °C to ensure adequate polymer melting, avoid thermal degradation, and ensure homogeneous dispersion of AA2024 particles within the PETG matrix. The screw rotation speed was carefully controlled to maintain stable material flow and sufficient shear mixing while minimizing particle agglomeration and excessive air entrapment. Continuous air cooling was applied immediately after extrusion to stabilize the filament geometry and maintain the nominal filament diameter of 1.75 mm. Filament feeding consistency and dimensional stability were continuously monitored during winding to avoid extrusion fluctuations during subsequent FDM printing. Excessively long thermal residence times were avoided to minimize thermal degradation of the PETG matrix. Additionally, the screw rotation rate was varied from 40 to 60 rpm to optimize shearing mixing without damaging PETG. Careful control of filament preparation parameters was necessary to ensure uniform reinforcement distribution and stable printability during FDM processing. Moisture removal prior to extrusion also minimized void formation and improved interfacial bonding between PETG and AA2024 particles. The filament diameter was measured continuously throughout the process using a KEYENCE LS-7030 laser micrometer (Keyence Corporation, Osaka, Japan), and the tolerance limit was kept within ±0.05 mm. After the extrusion process, the filaments were wound onto a roller, and several tests were conducted, including a surface test to detect irregularities, filament diameter testing, and filament flexibility testing. In case of any irregularities, such as voids, material fragility, or filament diameters exceeding the tolerance limit, the filaments were rejected. The characteristics of raw materials used in this experiment are provided in Table 1.

2.3. Fused deposition modeling printing process

The composite specimens were fabricated using a Bambu Lab A1 FDM 3D printer (Bambu Lab, China) equipped with a 0.4 mm brass nozzle. The printer was set up to work in a temperature range favorable for PETG composite materials. The printer nozzle temperature was varied between 230 °C and 250 °C, while the bed temperature was maintained around 80 °C to allow layer adhesion and prevent warping. The experiments were conducted using the design of experiments (DoE) method to investigate how different process variables affect the mechanical properties of the printed composite. The major parameters analyzed in this study included layer height (0.1 mm, 0.2 mm, and 0.3 mm), infill density (60%, 80%, and 100%), and nozzle temperature (230 °C, 240 °C, and 250 °C). The experimental plan in the present work was based on a Taguchi design to systematically investigate the influence of reinforcement concentration and FDM processing parameters on the composite performance characteristics. The selected parameter combinations enabled efficient evaluation of multiple processing variables while minimizing the total number of experimental trials. The adopted design framework also facilitated subsequent multi-criteria optimization using the hybrid AHP–TOPSIS approach. The raster angle was fixed at ±45° to enhance the isotropy of the sample, while the printing speed was kept constant at 50 mm/s. The CAD models were sliced using Bambu Handy software (version 3.0, Bamby Lab), with constant parameters such as shell thickness, number of perimeters, and cooling rate applied to all specimens printed in the experiments. These specimens were then cooled to room temperature and later detached from the platform to prevent distortion caused by residual stresses. The process parameters used for the experiment designs in this study are presented in Table 2. To determine the impact of process parameters, the print speed, bed temperature, and raster angle were held constant throughout the experiment because they have little effect on the FDM-fabricated composite.

Table 1. Physical and compositional properties of PETG and AA2024 powder used in this study

Material	Property	Value	Unit
PETG	Density	1.27	g/cm^3
	Glass transition temperature	75–85	°C
	Filament diameter	1.75 ± 0.05	mm
	Melt flow index	6–10	g/10 min
AA2024 powder	Purity	>99	wt.%
	Particle size	10–50	μm
	Morphology	Irregular to semi-spherical	-
	Major elements	Al–Cu–Mg	-

Abbreviation: PETG: Polyethylene terephthalate glycol

Table 2. FDM process parameters and levels used for experimental investigation

Parameter	Level 1	Level 2	Level 3	Unit
Layer height	0.1	0.2	0.3	mm
Infill density	60	80	100	%
Nozzle temperature	230	240	250	°C
Print speed (constant)	50	-	-	mm/s
Bed temperature (constant)	80	-	-	°C
Raster angle (constant)	±45	-	-	°

Abbreviation: FDM: Fused deposition modeling.

All specimens were fabricated using a flat build orientation to minimize geometric instability and maintain consistency across all experimental runs. The number of walls per perimeter was kept constant throughout the study to reduce variability in shell strength contributions. Cooling fan operation was controlled at a moderate level to ensure sufficient solidification while minimizing excessive thermal gradients that could weaken interlayer bonding. Printing was conducted under ambient chamber conditions without external chamber heating. These parameters were maintained constant throughout the experiments to isolate the effects of reinforcement concentration and primary FDM processing variables on composite performance.

2.4. Mechanical testing

Mechanical testing of the fabricated composite specimens was performed using a Tinius Olsen universal testing machine (Tinius Olsen Testing Machine Company, United States of America [USA]) in accordance with the relevant ASTM standards. Specifically, tensile testing was conducted according to ASTM D638 standards, using type V specimens whose dimensions followed the standard criteria. The universal testing machine was fitted with a load cell capable of handling the load, with a crosshead speed of 5 mm/min. The flexural properties of the composites were determined using three-point bend testing according to ASTM D790 criteria, with a support span-to-depth ratio of 16:1 and a loading rate of 2 mm/min. The compression tests were conducted in accordance with ASTM D695, and the specimens were subjected to uniaxial compressive force until failure. In each of the above tests, at least five specimens were used, and the results were reported as mean ± standard deviation. All the tests were performed at room temperature (25 °C). The stress-strain response, modulus of elasticity, ultimate strength, and failure modes of the materials were documented to determine the effects of AA2024 percentage and processing parameters on mechanical behavior. A summary of the test method and the responses considered during optimization is shown in Table 3.

Table 3. Experimental factors and response parameters used for analysis and optimization

Category	Parameter	Type	Unit
Material	AA2024 content	Input	wt.%
Process	Layer height	Input	mm
Process	Infill density	Input	%
Process	Nozzle temperature	Input	°C
Mechanical	Tensile strength	Output	MPa
Mechanical	Flexural strength	Output	MPa
Mechanical	Compression strength	Output	MPa
Tribological	Wear rate	Output (minimize)	Mm^3/N·m
Quality	Printability	Output (qualitative)	-
Quality	Dimensional accuracy	Output (qualitative)	-

2.5. Wear testing

The tribological properties of the fabricated composites were evaluated using a DUCOM TR-20LE pin-on-disc tribometer (DUCOM Instruments Pvt. Ltd., India) in accordance with ASTM G99 standards. Pin-shaped specimens were machined from the printed components, with dimensions appropriate for conducting the test. The counterpart disc was made of hardened steel with a definite surface roughness. Testing was carried out in the absence of lubrication under a constant normal force (10 N), a sliding speed of 1 m/s, and a sliding distance of 1,000 m. Wear rate was determined using the volume loss method, as follows:

$$Wear\,rate = \frac{Initial\,mass - Final\,mass}{Density \times Sliding\,distance \times Applied\,load} \quad (1)$$

Prior to the wear test, the specimens were cleaned with ethanol to remove contamination, and post-test cleaning was performed to determine the exact mass loss using an analytical balance. The friction coefficient was measured during the process to assess friction characteristics. The wear characteristics of the surfaces after the test were examined for various wear modes, including abrasive wear, adhesive wear, and delamination.

2.6. Microstructural analysis

Microstructural characterization of the fabricated composites was carried out using a JEOL JSM-IT200 scanning electron microscope (SEM; JEOL Ltd., Japan) to examine the dispersion of AA2024 particles, particle–matrix interaction, and fracture morphology of the composite specimens. Fractured samples resulting from mechanical testing procedures were coated with a thin film of gold to increase electrical conductivity and avoid charging effects when viewed under SEM. The SEM images were acquired at different magnifications to observe particle dispersion, void development, and crack formation at both macroscopic and microscopic scales. Special emphasis was placed on detecting particle pullout, debonding, and agglomeration, which have an impact on the mechanical properties of the composite material. Energy-dispersive spectroscopy (EDS) and SEM were used for analyzing elemental composition and distribution in the PETG matrix. The elemental mappings produced were used to analyze homogeneity in particle distribution by degree of reinforcement. A comprehensive summary of the fabrication parameters, experimental conditions, and corresponding performance properties evaluated during the present investigation is provided in Table 4.

2.7. Multi-criteria decision-making optimization framework

To identify the optimal combination of material and process characteristics, the following MCDM procedure and AHP–TOPSIS techniques were used. In the first step, AHP was applied to evaluate the criteria weights. They reflect the relative importance of performance indicators: tensile strength, flexural strength, compression strength, wear rate (minimization criterion), and quality attributes such as printability and dimensional accuracy. Pairwise comparisons were used to construct the comparison matrix according to Saaty's scale, and its consistency ratio (CR) was calculated to check the logical consistency of the judgments ($CR < 0.1$). The weights of the criteria were derived by calculating the normalized eigenvector corresponding to the largest eigenvalue. In the second step, TOPSIS was utilized to select the optimal alternative among the experimental combinations of materials and process settings. A decision matrix was formulated based on the normalized experimental data. Then, the data were multiplied by the criteria weights determined in step 1. The positive ideal solution (with the best values) and the negative ideal solution (with the worst values) were defined, and the Euclidean distance of each alternative to these reference points was determined. The coefficient of relative nearness was calculated, and the alternatives were ranked using it, with the alternative with the maximum coefficient considered the best.

Table 4. Summary of fabrication parameters and measured properties used in the experimental investigation

Experimental parameter	Levels/Conditions	Property evaluated
AA2024 reinforcement content	0 wt.%, 2.5 wt.%, 5 wt.%, 7.5 wt.%	Tensile strength, flexural strength, compressive strength, wear resistance, dimensional accuracy
Layer height	0.1 mm, 0.2 mm, 0.3 mm	Surface quality, dimensional accuracy, mechanical properties
Infill density	60%, 80%, 100%	Tensile strength, compressive strength, wear behavior
Nozzle temperature	230 °C, 240 °C, 250 °C	Interlayer bonding, print quality, mechanical performance
Raster angle	±45° (constant)	Structural uniformity
Print speed	50 mm/s (constant)	Printing consistency
Bed temperature	80 °C (constant)	Layer adhesion and warpage control
Build orientation	Flat orientation (constant)	Geometric stability and repeatability
Cooling fan setting	Moderate cooling (constant)	Layer solidification and bonding stability

The integrated AHP–TOPSIS framework enabled the simultaneous evaluation of multiple conflicting performance criteria and provided a systematic decision-making methodology for optimizing the fabricated PETG/AA2024 composite system.

Printability was quantitatively evaluated based on extrusion continuity, the absence of nozzle clogging, layer deposition consistency, and the occurrence of visual defects during specimen fabrication. Dimensional accuracy was assessed by comparing the measured dimensions of printed specimens with their corresponding CAD dimensions using digital Vernier calipers. The dimensional deviation percentage was calculated for each specimen and incorporated into the multi-criteria optimization framework. A flowchart of the steps for implementing the proposed hybrid multi-objective optimization method is shown in Figure 2.

2.8. Closeness coefficient calculation

To calculate the closeness coefficient, **Equation 2** was used:

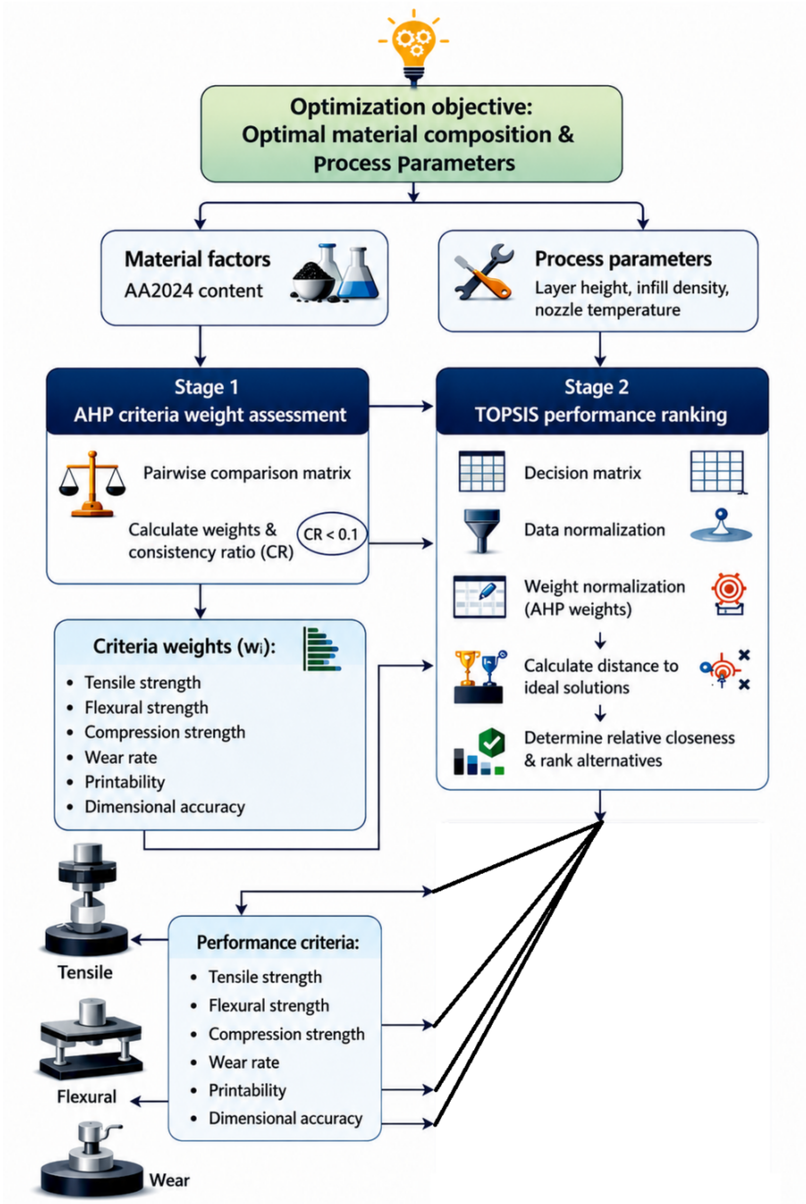

Figure 2. Flowchart of the hybrid analytical hierarchy process–technique for order preference by similarity to ideal solution (AHP–TOPSIS) multi-criteria decision-making framework used for the optimization of material composition and fused deposition modeling (FDM) process parameters, highlighting criteria weight determination using AHP and performance ranking based on TOPSIS

$$CC_i = \frac{S_i^-}{S_i^+ + S_i^-} \quad (2)$$

where CC_i represents the closeness coefficient of the ith alternative, S_i^+ denotes the separation distance from the positive ideal solution, and S_i^- represents the separation distance from the negative ideal solution.

2.9. Statistical analysis

The pairwise comparison analysis required for the AHP was performed using Microsoft Excel 2021 (Microsoft Corporation, USA). The comparison matrix was developed according to Saaty's nine-point scale, and the relative weights of the evaluation criteria were determined from the normalized principal eigenvector. The consistency of expert judgments was assessed through the calculation of the consistency index and consistency ratio. A consistency ratio value less than 0.10 (CR < 0.10) was considered acceptable, indicating satisfactory logical consistency of the pairwise comparisons. The weighted criteria obtained from the AHP analysis were subsequently incorporated into the TOPSIS model for ranking the experimental alternatives. Statistical analysis of the experimental results was performed using Minitab® Statistical Software Version 21.1 (Minitab LLC, USA). The reported values represent the mean ± standard deviation obtained from five independent specimens for each experimental condition. Statistical significance was evaluated at a confidence level of 95%, corresponding to an alpha value of 0.05 ($p < 0.05$).

3. Results and discussion

For each experimental condition, multiple specimens were tested, and the reported values were mean ± standard deviation to indicate experimental variability and repeatability.

3.1. Mechanical properties

A detailed investigation on the mechanical and tribological properties of AA2024-filled PETG materials prepared through the FDM process was carried out to determine the effect of filler loading on material performance. The results conclusively show that the addition of AA2024 particles to PETG considerably improved the performance of the base polymer, reaching an optimum level above which further increases in filler loading lead to some degradation. Compared with pure PETG, adding metal particles improved the stiffness, strength, and wear resistance of the material through effective stress transfer. The reinforcement concentrations of 0, 2.5, 5, and 7.5 wt.% were selected based on preliminary extrusion trials and previous literature related to metal-filled polymer composites fabricated through FDM. Lower reinforcement levels were expected to improve particle dispersion and printability, whereas excessively high filler concentrations may promote particle agglomeration, increased melt viscosity, nozzle clogging, poor interlayer bonding, and dimensional instability during printing. Therefore, the selected concentration range was considered appropriate for balancing reinforcement effectiveness and process stability.

3.1.1. Tensile strength

The tensile strength gradually increased from 0 to 5 wt.% AA2024 addition, followed by a marginal drop thereafter (Table 5). Pure PETG had a tensile strength of 49.5 ± 1.2 MPa. When reinforced at 2.5 wt.%, the tensile strength was 54.8 ± 1.4 MPa (+10.7%). At 5 wt.%, the tensile strength reached its peak value of 59.3 ± 1.3 MPa (+19.8% relative to the base material). The observed improvement may be associated with improved stress transfer capability and enhanced particle–matrix interactions resulting from a relatively uniform AA2024 particle distribution within the PETG matrix. Since the metal particles were evenly distributed throughout the PETG matrix, they provided strong points of reinforcement for the composite materials, limiting the movement of polymer chains while increasing stress tolerance. The particles also help deflect cracks and dissipate energy during deformation, thus postponing failure. On the other hand, when the loading reached 7.5 wt.%, the tensile strength dropped to 56.1 ± 1.6 MPa (+13.3%). This observation was mainly due to particle agglomeration and microvoid creation, which concentrate stress at specific points and disrupt interface bonding. This trend is in agreement with other literature sources reporting on the mechanical behavior of aluminum-alloyed polymer composite materials, where peak mechanical properties are attained at medium concentrations of fillers.[17-20]

Table 5. Tensile strength of AA2024-reinforced PETG composites at different weight fractions

AA2024 (wt.%)	Tensile strength (MPa)	Change vs. Neat PETG (%)
0	49.5 ± 1.2	-
2.5	54.8 ± 1.4	+10.7
5	59.3 ± 1.3	+19.8
7.5	56.1 ± 1.6	+13.3

Abbreviation: PETG: Polyethylene terephthalate glycol.

3.1.2. Flexural strength

Flexural strength showed a similar trend to tensile behavior, with a considerable increase up to an optimum filler content (Table 6). The flexural strength of the neat PETG sample was 76.2 ± 1.5 MPa. Meanwhile, the flexural strength of the material reinforced by 2.5 wt.% of AA2024 increased to 81.9 ± 1.7 MPa (+7.5%), demonstrating enhanced bending resistance. Optimum content of the reinforcing filler of 5 wt.% resulted in the highest flexural strength of 89.6 ± 1.4 MPa (+17.6%), attributed to the metallic fillers' role in enhancing the composite's bending resistance. A higher elastic modulus of metal particles increases their contribution to bearing loads, reducing composite deformability. In addition, homogeneous filler distribution promotes efficient transfer of stresses through the material. Meanwhile, with an increase in filler content to 7.5 wt.%, flexural strength decreased to 84.3 ± 1.6 MPa (+10.6%). These results are consistent with other studies reporting deterioration in mechanical performance with the addition of further filler, due to poor dispersion and a high concentration of defects.[21-23]

Table 6. Flexural strength of AA2024-reinforced PETG composites

A2024 (wt.%)	Flexural strength (MPa)	Change vs. Neat PETG (%)
0	76.2 ± 1.5	-
2.5	81.9 ± 1.7	+7.5
5	89.6 ± 1.4	+17.6
7.5	84.3 ± 1.6	+10.6

Abbreviation: PETG: Polyethylene terephthalate glycol.

3.1.3. Compression strength

The compression strength of the composites displayed a progressive increase upon AA2024 inclusion, peaking at 5 wt.% content (Table 7). The neat PETG had a compressive strength of 62.0 ± 2.1 MPa, which increased by 10.8% to 68.7 ± 1.8 MPa at 2.5 wt.% and rose further by 20.2% to 74.5 ± 1.6 MPa at 5 wt.%. This increase in compressive strength was mainly attributed to the natural rigidity of AA2024 particles, which hinders their deformation and thus enables load transfer during compression. The inclusion of rigid particles in the matrix hampers its compressibility and improves its structural integrity. However, an increase in filler concentration to 7.5 wt.% led to a slight decrease in compressive strength to 72.2 ± 2.0 MPa (+16.4%). This could have been due to particle agglomeration and the formation of stress-concentration zones, preventing further improvements in mechanical performance. These findings corroborated studies on metal-filled polymer composites, in which the optimal filler content maximized compressive strength before saturating the system.[24-27]

Table 7. Compression strength of AA2024-reinforced PETG composites

AA2024 (wt.%)	Compression strength (MPa)	Change vs. Neat PETG (%)
0	62.0 ± 2.1	-
2.5	68.7 ± 1.8	+10.8
5	74.5 ± 1.6	+20.2
7.5	72.2 ± 2.0	+16.4

Abbreviation: PETG: Polyethylene terephthalate glycol.

3.1.4. Wear rate

Tribological behavior of the composites was analyzed by measuring the wear rate, which decreased significantly with increasing AA2024 content up to 5 wt.% (Table 8). The wear rate of pure PETG was 0.042 mm^3/N·m, indicating its relatively high sensitivity to mechanical surface degradation. With the addition of 2.5 wt.% of metallic particles, the wear rate reduced to 0.031 mm^3/N·m (−26.2%). The decrease in wear rate is due to the particles' ability to form a protective layer and act as microbarriers, thereby preventing loss of composite material. Further increase of reinforcement to 5 wt.% led to a wear rate of 0.025 mm^3/N·m (−40.5%), indicating that this composite exhibits the highest tribological properties among all tested composites. Increasing the particle concentration to 7.5 wt.% increased the wear rate slightly to 0.028 mm^3/N·m (−33.3%). Such a result can be explained by the uneven distribution of fillers and by weak adhesion between their surfaces and the matrix, leading to particle pullout from the matrix surface. As shown by the results, uniform filler dispersion plays a vital role in reducing wear rate.[28-30]

Table 8. Wear rate of AA2024-reinforced PETG composites under dry sliding conditions

AA2024 (wt.%)	Wear rate (mm^3/N·m)	Change vs. Neat PETG (%)
0	0.042	-
2.5	0.031	−26.2
5	0.025	−40.5
7.5	0.028	−33.3

Abbreviation: PETG: Polyethylene terephthalate glycol.

Figure 3 demonstrates the effect of filler fraction on the mechanical and tribological characteristics of AA2024/PETG composite materials. It can be seen that the tensile, flexural, and compression strengths steadily increased with increasing AA2024 percentage until reaching 5 wt.%, after which a decrease was observed at 7.5 wt.%. The tensile strength varied from 49.5 MPa for pure PETG to 59.3 MPa at 5 wt.%, the flexural strength increased from 76.2 MPa to 89.6 MPa, and the compression strength increased from 62.0 MPa to 74.5 MPa. This behavior is explained by efficient load transfer resulting from the dispersion of filler particles and the restriction of polymer chain motion within the composite, both of which increase its stiffness. Meanwhile, with the higher filler fraction of 7.5 wt.%, a decrease in strength is observed due to agglomeration and the formation of defects that can act as stress concentrators.

In contrast, the wear rate showed the opposite behavior, with a considerable drop from 0.042 $mm^3/N{\cdot}m$ in pure PETG to 0.025 $mm^3/N{\cdot}m$ in 5 wt.% AA2024, thus resulting in improved resistance against material wear due to friction. The improved wear resistance observed at intermediate reinforcement levels may be associated with reduced material removal and improved load-bearing capability of the composite surface. Possible contributions from tribological surface-layer formation are consistent with the literature; however, detailed worn-surface characterization was not conducted in the present work. At 7.5 wt.%, an increase in the wear rate was observed, attributed to particle nonuniformity and particle pullout. From the figure, it is evident that 5 wt.% AA2024 showed an optimum performance in terms of strength and wear resistance.

3.2. Microstructural analysis

The microstructure analysis conducted using SEM yielded important findings on the dispersion of AA2024

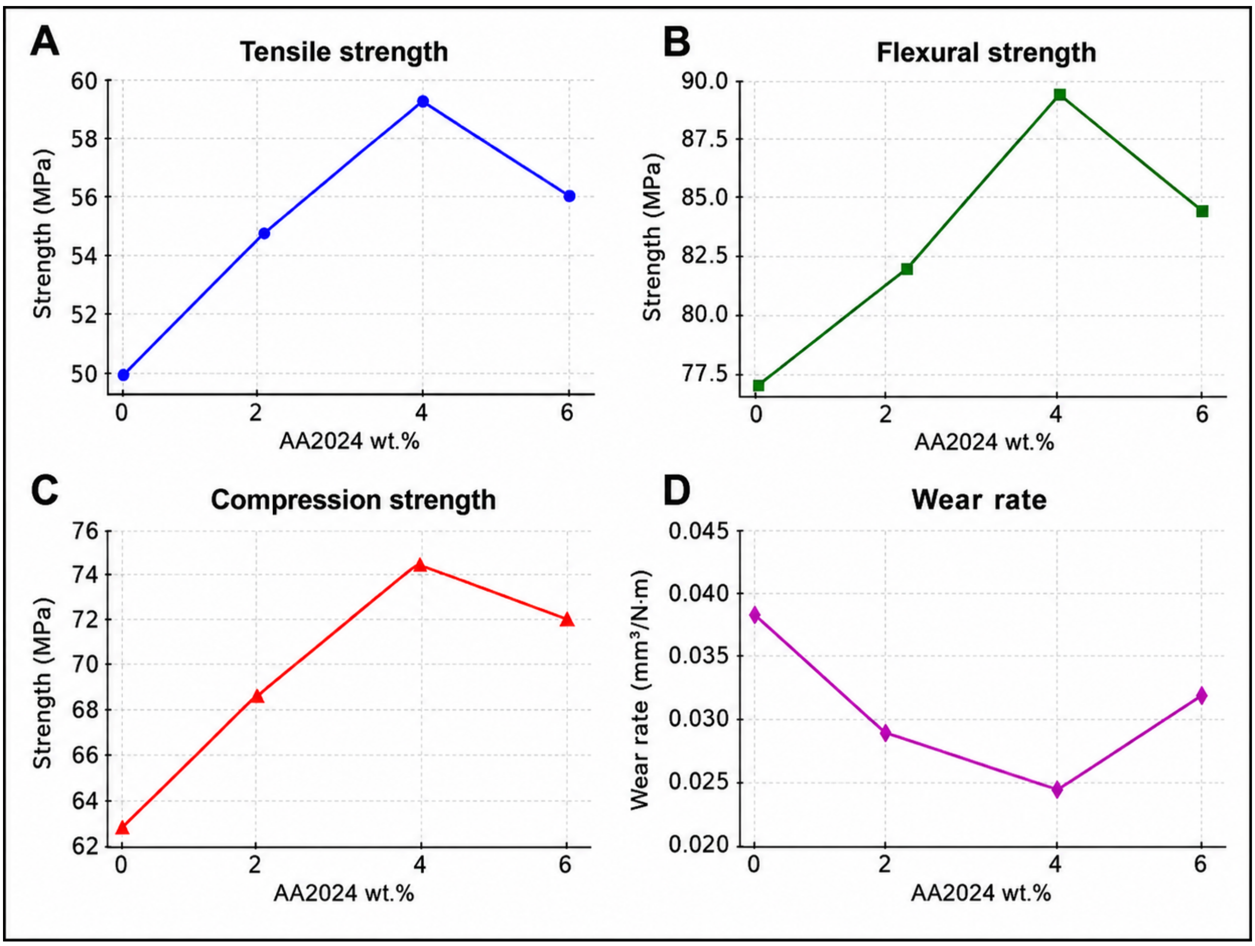

Figure 3. Effect of AA2024 weight fraction on (A) tensile strength, (B) flexural strength, (C) compression strength, and (D) wear rate of polyethylene terephthalate glycol (PETG) composites fabricated via fused deposition modeling (FDM)

particles and their effect on the performance of the composite material. The surface of pure PETG showed a smooth surface, with elongated fibers associated with ductile fracture. Conversely, the surfaces of the composite materials containing 2.5 wt.% and 5 wt.% of AA2024 had a somewhat different structure, with particles uniformly distributed within the matrix. This is a clear indication of strong bonding between the two components, promoting efficient load transfer and thus improving mechanical properties. At 7.5 wt.% of AA2024, SEM images indicated particle agglomeration, microvoids, and interfacial debonding. Such defects can serve as crack-nucleation centers, leading to early fractures and inferior mechanical behavior. In addition, EDS analysis results proved the existence of aluminum, copper, and magnesium, consistent with AA2024, thus confirming the successful introduction of the metallic phase into the structure. It can be seen that at lower loadings, reinforcement was uniformly distributed, whereas at higher loadings, it was clustered, thereby contributing to poor mechanical behavior.[31-33] Figure 4 illustrates changes in reinforcement dispersion, interfacial bonding, and defect development with increasing AA2024 concentrations. The mechanical behavior suggests that the selected reinforcement level promoted favorable interaction between the PETG matrix and AA2024 particles, although detailed interfacial characterization was beyond the scope of the present study.

3.3. Optimization using analytical hierarchy process–technique for order preference by similarity to ideal solution

A hybrid methodology combining AHP and TOPSIS was used to determine the optimal combination of material composition and FDM processing parameters. The considered criteria were tensile strength, bending strength, compressive strength, wear rate (as a minimization criterion), and subjective attributes such as printability and dimensional accuracy. Using the AHP, relative weights for each criterion were assigned based on their priority to ensure equal consideration of mechanical and functional properties. The CR was kept within an acceptable range to ensure consistent judgments. In addition, the TOPSIS

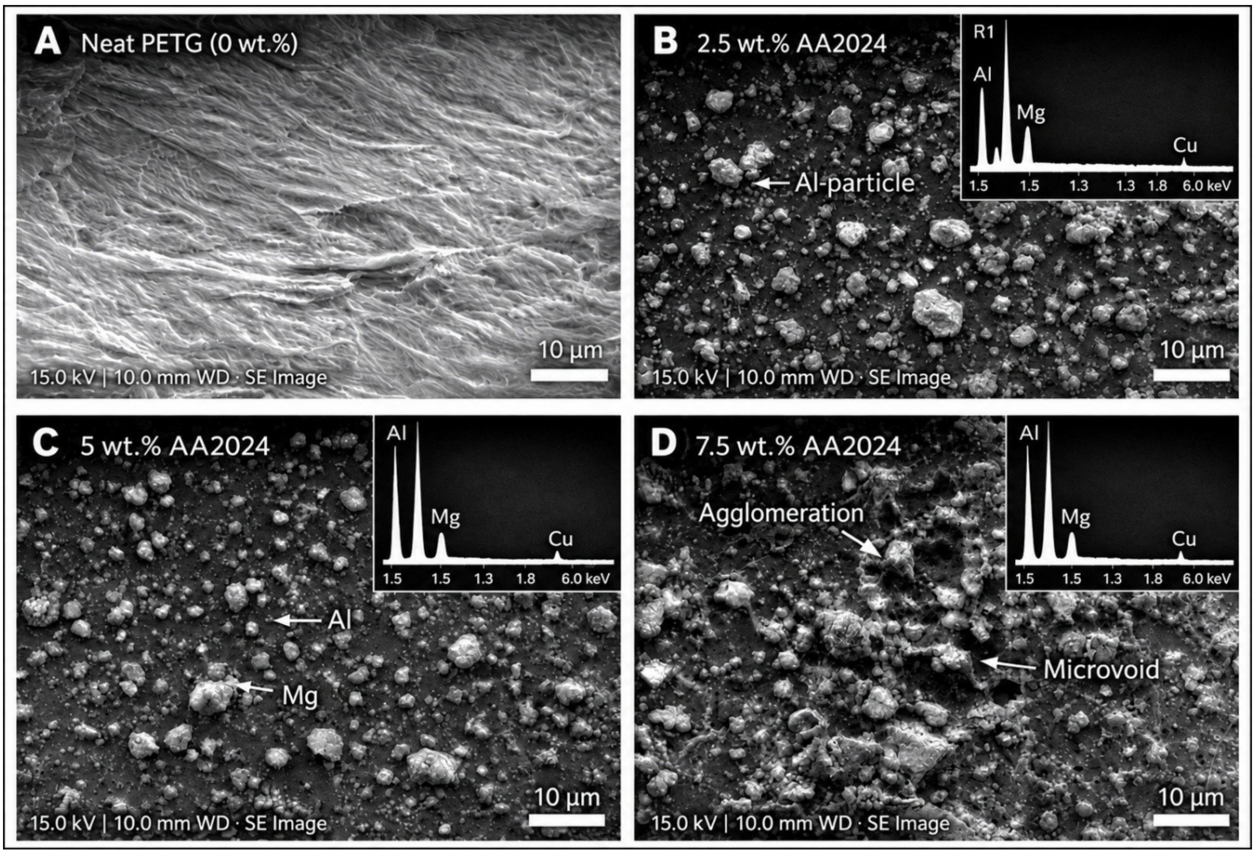

Figure 4. Scanning electron microscopy (SEM) micrographs of AA2024-reinforced polyethylene terephthalate glycol (PETG) composites at (A) 0 wt.%, (B) 2.5 wt.%, (C) 5 wt.%, and (D) 7.5 wt.% showing particle dispersion, interfacial bonding, and agglomeration. EDS insets confirm the presence of Al, Mg, and Cu elements. Scale bars: 10 µm; magnifications: 3,000×.

method was applied by developing a normalized decision matrix and calculating the Euclidean distances between the alternatives and the ideal and negative-ideal solutions. According to the findings, the set of parameters with a 0.2 mm layer thickness, 80% infill percentage, 240°C extruder temperature, and 5 wt.% AA2024 alloy resulted in the highest TOPSIS score of 0.857. The combination thus represents an optimal balance among these three attributes. This demonstrates the need for integrating optimization methods into additive manufacturing. Table 9 presents the ranking of parameter combinations obtained using the AHP–TOPSIS technique.

The sensitivity of the developed optimization approach based on the hybrid AHP–TOPSIS model was tested by changing the weights of the decision criteria (±10–20%), with the CR remaining below the threshold (CR < 0.1). The starting weights given to each criterion by the AHP approach were: tensile strength (0.28); flexural strength (0.22); compression strength (0.20); wear rate (0.18); and printability and dimensional accuracy (0.12). When the weight of individual criteria was changed, the ranks given by the TOPSIS approach showed minimal fluctuations, with the optimum configuration of parameters (5 wt.% AA2024, 0.2 mm layer height, 80% infill, and 240 °C nozzle temperature) being consistently ranked either first or second with minor changes in closeness coefficient (±0.015).

The proposed model was tested against single-criterion optimization models and other MCDM models available in the literature.[34,35] The results showed that, unlike single-criterion optimization models, which focused only on maximum strength or minimum wear, the AHP–TOPSIS model produced better solutions when both criteria were optimized simultaneously. The proposed model outperformed other models, such as the weighted-sum method and gray relational analysis (GRA) models, owing to its better discriminating power. This is evident from the range of TOPSIS scores (0.712–0.857) obtained by the model.

The optimized parameter set was verified using confirmation experiments under the predicted optimal conditions. There was no significant difference between the predicted and experimental values; only a deviation of ±3% for mechanical properties and ±5% for wear rate. Thus, the model's predictive accuracy is high. The optimal *set al*ways provided better results than non-optimal sets.

Reliability analysis was performed through assessing repeatability and statistical stability between multiple experiments. Low standard deviation values were obtained for all studied material properties (no more than 2 MPa for tensile strength and no more than 0.003 mm^3/N·m for wear). Moreover, a stable ranking order between successive TOPSIS analyses also proved the reliability of the proposed method. Thus, the reliability, accuracy, and robustness of the applied hybrid AHP–TOPSIS approach were demonstrated.

3.4. Correlation between microstructure and properties

In this work, a correlation between microstructural parameters and macroproperties was successfully drawn. The even dispersion of AA2024 powder particles at 5 wt.% improved interfacial bonding, decreased the number of voids, and optimized load transfer, thus contributing to excellent mechanical and tribological properties. However, when the amount of filler reached 7.5 wt.%, agglomeration of particles, defects, and weak interfacial areas were observed, which had a detrimental effect on the properties of the specimens tested. This clearly shows that the processing method and material should be carefully controlled to attain optimal results. It is worth mentioning that combining experimental research with an

Table 9. Ranking of parameter combinations based on AHP–TOPSIS analysis

Rank	AA2024 (wt.%)	Layer height (mm)	Infill density (%)	Nozzle temp (°C)	TOPSIS score
1	5	0.2	80	240	0.857
2	5	0.2	100	240	0.821
3	2.5	0.2	80	240	0.794
4	7.5	0.2	80	240	0.768
5	0	0.2	80	240	0.712

Abbreviation: AHP: Analytical hierarchy process; TOPSIS: Technique for order preference by similarity to ideal solution.

optimization approach allows for establishing correlations between the processing, structure, and properties.

Overall, the findings from the investigation provide convincing evidence of a direct correlation between processing, microstructure, properties, and performance for AA2024-reinforced PETG composite samples produced using FDM technology. Specifically, all tested parameters (tensile strength, flexural strength, compression strength, and wear resistance) have a non-linear dependence on reinforcing agent concentration; however, the best combination of all parameters was observed at the optimal concentration level equal to 5 wt.%, which means that further increase in AA2024 concentration leads to a decrease in material performance. This phenomenon can be explained by a change in the microstructure of the material; more specifically, at low concentrations (2.5–5 wt.%), the uniform distribution of AA2024 particles promotes improved interfacial interactions and efficient stress transfer, thus enhancing stiffness and reducing the likelihood of crack nucleation. Also, incorporating hard aluminum alloy particles improves surface integrity by reducing ploughing and cutting, thereby significantly decreasing the wear rate. Nevertheless, above the optimal amount (7.5 wt.%), interactions between particles become dominant over those between the matrix and particles; therefore, agglomeration occurs, creating microvoids that lead to interfacial debonding and act as stress concentrations for premature failure of the material. It demonstrates the importance of achieving the proper reinforcement/matrix ratio for polymer-metal composites processed by FDM.

In summary, the AHP–TOPSIS-based optimization methodology enables the identification of the optimal combination of composite material properties and technological process parameters from a holistic perspective. The use of MCDM (mechanical strength, wear resistance, and manufacturability of the fabricated parts) helps overcome the drawbacks of a single-criterion optimization approach, making the proposed model closer to reality. The optimal design identified (5 wt.% AA2024, 0.2 mm layer thickness, 80% infill density, and 240 °C nozzle temperature) implies an appropriate amount of thermal energy for layer bonding, proper material consolidation, and control of the internal microstructure of the specimens. The robustness of the proposed weighting factors and ranking order was verified using the sensitivity analysis of the results. Finally, the high accuracy of the prediction proves the efficiency of the proposed modeling technique.

However, some limitations remain despite the positive results. Firstly, the experiments were conducted using a limited number of fillers and processing conditions, which might not represent the full scope of the design of FDM composite materials. Secondly, although microparticles are easier to process, their use limits the interface surface area compared with nanoscale reinforcement, thus limiting the potential to improve the material's properties. Thirdly, there was little research on the anisotropy of the printed part, as the raster angle and orientation remained constant throughout the process. Fourthly, although the microstructural investigation provided valuable information, it was primarily qualitative. To gain additional insights, micro-computed tomography or image analysis should be used. Lastly, fatigue, creep, and degradation resistance were not studied in this paper.

Further investigations could aim to overcome the aforementioned constraints by expanding the parameter space and developing innovative hybrid reinforcement schemes, such as combining metal particles with nano-fillers and applying surface treatments to improve interfacial compatibility between the components. It could be beneficial to implement surface-functionalization treatments to improve the interaction between filler particles and the polymer matrix and to overcome particle agglomeration at high filler concentrations. More advanced methods of in situ measurements and numerical simulation studies, such as finite element analyses and machine learning-based models, may allow for better prediction of the process-structure-property relations in such systems. Moreover, an examination of various build orientations and multi-component printing strategies could give an insight into the anisotropic properties of the investigated composite system. Lastly, a broader range of tests, including fatigue-strength and thermal-stability measurements, as well as application studies in industrial settings, would be necessary for implementing such systems in practice.

4. Conclusion

The developed AA2024-reinforced PETG composite demonstrates promising mechanical and tribological performance for advanced FDM applications. Although additive manufacturing may offer advantages related to material utilization efficiency and reduced material waste, detailed environmental and sustainability assessments were beyond the scope of the present study. The addition of AA2024 filler particles considerably increased the mechanical and tribological properties of PETG, with the tensile strength, flexural strength, and compression strength improved by 19.8%, 17.6%, and 20.2%, respectively, while wear resistance was enhanced by 40.5%. According to microscopic studies, these enhancements were mainly due to uniform dispersion and strong interfacial bonding, ensuring effective load transfer and deformation resistance. Nonetheless, higher filler addition (7.5 wt.%) led to agglomeration and microvoid formation, slightly reducing their performances.

The optimum composition of the material, along with the corresponding process parameters based on the AHP–TOPSIS approach, was 5 wt.% AA2024, a layer thickness of 0.2 mm, an infill density of 80%, and a nozzle temperature of 240 °C. This composition yielded the maximum performance due to optimized values of strength, wearability, and printability. The successful implementation of the above method demonstrates that AHP–TOPSIS can be used effectively to optimize additive manufacturing processes involving complex materials.

Future work should focus on improving compatibility among layers by modifying the surfaces of metallic powders, using advanced microstructure characterization tools, studying other alloy systems, and considering hybrid reinforcements. Additionally, machine learning algorithms and numerical simulations could be utilized to improve composite prediction.

Acknowledgments

None.

Funding

This project is sponsored by Prince Sattam Bin Abdulaziz University (PSAU) as part of funding for its PSAU Global South Partnership (GSP), under project number PSAU-GSP-RDFP-2025-0113.

Conflict of interest

The authors declare that there is no conflict of interest regarding the publication of this paper.

Author contributions

Conceptualization: Raja Subramani, Mohamad Reda A. Refaai
Data curation: Raja Subramani
Formal analysis: Rajeswari Nageswaran, Mukhtar Fatihu Hamza
Funding acquisition: Mohamad Reda A. Refaai
Investigation: Raja Subramani, Jaiprakash Narain Dwivedi
Methodology: Raja Subramani, Babatunde Omoniyi Odedairo
Project administration: Mohamad Reda A. Refaai
Resources: Saad Rashed Alquraini
Software: Jaiprakash Narain Dwivedi
Supervision: Mohamad Reda A. Refaai
Validation: Rajeswari Nageswaran, Saad Rashed Alquraini, Babatunde Omoniyi Odedairo
Visualization: Rajeswari Nageswaran, Mukhtar Fatihu Hamza
Writing–original draft: Raja Subramani
Writing–review & editing: Mohamad Reda A. Refaai, Rajeswari Nageswaran, Babatunde Omoniyi Odedairo

Ethics approval and consent to participate

Not applicable.

Consent for publication

Not applicable.

Availability of data

Data are available upon reasonable request to the corresponding author.

References

1. Raja S, Iliyas AJM, Vishnu PS, *et al.* Sustainable manufacturing of FDM-manufactured composite impellers using hybrid machine learning and simulation-based optimization. *Mater Sci Addit Manuf.* 2025;4(3):025200033.

   doi: 10.36922/MSAM025200033

2. Khieng TK, Debnath S, Ting Chaw Liang E, *et al.* A review on mechanical properties of natural fibre reinforced polymer composites under various strain rates. *J Compos Sci.* 2021;5(5):130.

   doi: 10.3390/jcs5050130

3. Khan A, Saxena KK. A review on enhancement of mechanical properties of fiber reinforcement polymer composite under different loading rates. *Mater Today Proc.* 2022;56:2316-2322.

   doi: 10.1016/j.matpr.2021.12.009

4. Mahesh V, Hadi P, Mahesh V. Machine learning-assisted optimization of FFF parameters for enhanced dimensional accuracy in PETG and CF-PETG composites. *J Mater Eng Perform.* 2026:1-19.

   doi: 10.1007/s11665-026-13416-x

5. Loknath D, Vakkalagadda MRK. Mechanical performance and interlayer adhesion of multi-material 3D-printed PETG/PETG-carbon-fiber composites. *Compos Interfaces.* 2025:1-18.

   doi: 10.1080/09276440.2025.2602996

6. Samaan KR, Alaa Eldin Sayed R, Atef M, *et al.* Mechanical and thermal optimization of fused deposition modeling of PETG and PETG-carbon-fiber composites. *J Thermoplast Compos Mater.* 2026:08927057261415790.

   doi: 10.1177/08927057261415790

7. Demir ME, Ergün RK. Mechanical and wear performance

of Al-, mica-, SiO2-filled glass fiber-reinforced composites and prediction of wear properties with artificial neural networks. *Proc Inst Mech Eng E J Process Mech Eng*. 2026;240(2):1243-1257.

doi: 10.1177/09544089241307840

8. Vinay DL, Keshavamurthy R, Tambrallimath V. Enhanced mechanical properties of metal filled 3D printed polymer composites. *J Inst Eng India Ser D*. 2023;104(1):181-195.

doi: 10.1007/s40033-022-00406-1

9. Vardhan H, Kumar R, Chohan JS. Investigation of tensile properties of sprayed aluminium based PLA composites fabricated by FDM technology. *Mater Today Proc*. 2020;33:1599-1604.

doi: 10.1016/j.matpr.2020.05.335

10. James DJD, Pandiyan GK, Vijay R, Vinod A, Sanjay MR, Suchart S. Chemically treated Acacia nilotica filler-reinforced epoxy composites: tribological studies and optimization of process parameters. *Chem Pap*. 2024;78(13):7395-7407.

doi: 10.1007/s11696-024-03601-4

11. Tanveer MQ, Mishra G, Mishra S, Sharma R. Effect of infill pattern and infill density on mechanical behaviour of FDM 3D printed parts—a current review. *Mater Today Proc*. 2022;62:100-108.

doi: 10.1016/j.matpr.2022.02.310

12. Akhoundi B, Behravesh AH, Bagheri Saed A. Improving mechanical properties of continuous fiber-reinforced thermoplastic composites produced by FDM 3D printer. *J Reinf Plast Compos*. 2019;38(3):99-116.

doi: 10.1177/0731684418807300

13. Omer MA, Shaban IA, Mourad AH, Hegab H. Advances in interlayer bonding in fused deposition modelling: a comprehensive review. *Virtual Phys Prototyp*. 2025;20(1):e2522951.

doi: 10.1080/17452759.2025.2522951

14. Singh V, Sharma SK. Applying hybrid approach of AHP, DEMATEL, and TOPSIS to study the impact of multiagent technology on the performance of manufacturing organizations. *IEEE Trans Eng Manag*. 2024;71:9299-9313.

doi: 10.1109/TEM.2023.3293948

15. Kitila LG, Duc E, Durieux S, Taddese GA. An integrated fuzzy AHP-fuzzy TOPSIS approach for multi-criteria decision-making framework in sustainable manufacturing process selection. *Int J Adv Manuf Technol*. 2026;142(1):559-583.

doi: 10.1007/s00170-025-16881-1

16. Al-Ibadi DJ, Ali HB, Sansarci ES. Hybrid manufacturing optimization using an analytic hierarchy method for multi-objective. *Iraqi J Mech Mater Eng*. 2024;23(1):74-91.

17. Kumar J, Negi S. Effect of additive manufacturing-based surface modification on pool boiling heat transfer: a review. *Prog Addit Manuf*. 2025;10(5):3225-3249.

doi: 10.1007/s40964-024-00820-9

18. Ahmed MM, El-Sayed Seleman MM, Fydrych D, *et al*. Friction stir welding of aluminum in the aerospace industry: the current progress and state-of-the-art review. *Materials*. 2023;16(8):2971.

doi: 10.3390/ma16082971

19. Karunakaran SK, Arumugam GM, Yang W, *et al*. Recent progress in inkjet-printed solar cells. *J Mater Chem A*. 2019;7(23):13873-13902.

doi: 10.1039/C9TA03155C

20. Zhu J, Abeykoon C, Karim N. Investigation into the effects of fillers in polymer processing. *Int J Lightweight Mater Manuf*. 2021;4(3):370-382.

doi: 10.1016/j.ijlmm.2021.04.003

21. Xu H, Gong LX, Wang X, *et al*. Influence of processing conditions on dispersion, electrical and mechanical properties of graphene-filled-silicone rubber composites. *Compos Part A Appl Sci Manuf*. 2016;91:53-64.

doi: 10.1016/j.compositesa.2016.09.011

22. Šupová M, Martynková GS, Barabaszová K. Effect of nanofillers dispersion in polymer matrices: a review. *Sci Adv Mater*. 2011;3(1):1-25.

doi: 10.1166/sam.2011.1136

23. Zaaba NF, Ismail H, Saeed AM. A review: metal filled thermoplastic composites. *Polym Plast Technol Mater*. 2021;60(10):1033-1050.

doi: 10.1080/25740881.2021.1882489

24. Adeniyi AG, Ighalo JO. A systematic review of pure metals reinforced plastic composites. *Iran Polym J*. 2021;30(7):751-768.

doi: 10.1007/s13726-021-00922-z

25. Zaaba NF, Ismail H, Saeed AM. A review: metal filled thermoset composites. *Polym Plast Technol Mater*. 2022;61(1):13-26.

doi: 10.1080/25740881.2021.1948058

26. Jaafar M. Development of hybrid fillers/polymer nanocomposites for electronic applications. In: *Hybrid Nanomaterials: Advances in Energy, Environment and Polymer Nanocomposites*. Hoboken, NJ: Wiley; 2017:349-369.

doi: 10.1002/9781119160380.ch7

27. Adeniyi AG, Emenike EC, Iwuozor KO, Saliu OD. Solvated polystyrene resin: a perspective on sustainable alternative to epoxy resin in composite development. *Mater Res Innov*. 2023;27(7):490-502.

doi: 10.1080/14328917.2023.2199597

28. Hao Y, Zhou X, Shao J, Zhu Y. The influence of multiple fillers on friction and wear behavior of epoxy composite coatings. *Surf Coat Technol*. 2019;362:213-219.

doi: 10.1016/j.surfcoat.2019.01.110

29. Sun W, Liu X, Liu K, Xu J, Wang W, Ye J. Paradoxical filler size effect on composite wear: filler–matrix interaction and its tribochemical consequences. *Tribol Lett*. 2020;68(4):131.

doi: 10.1007/s11249-020-01375-w

30. Buaksuntear K, Choosang N, Mougin K, *et al*. Recent advancements in masterbatch filler technology and filler dispersion for rubber and polymer composites: a review. *Polym Eng Sci*. 2026;66(3):1582-1610.

doi: 10.1002/pen.70338

31. Jierula A, Ding S, Liu H, Yang B. Damage evolution in different reinforcement configurations during four-point bending: acoustic emission analysis using K-means clustering. *J Nondestruct Eval*. 2026;45(1):40.

doi: 10.1007/s10921-026-01333-x

32. Navaneethasanthakumar S, Velmurugan S, Sugunarani S, Ramasundaram K. Enhancement of mechanical and tribological properties of AA5052 aluminium alloy via hybrid Si3N4/BN nanoparticle reinforcement using friction stir processing. *Compos Interfaces*. 2026:1-19.

doi: 10.1080/09276440.2026.2630147

33. Adhikesavan M, Dhairiyasamy R, Mottaiyan P, Singh S. Synergistic reinforcement strategies: nanosilica with graphene versus MoS2 in high-performance glass/epoxy composites. *J Mater Eng Perform*. 2026;35(10):10243-10266.

doi: 10.1007/s11665-025-12399-5

34. Chakraborty A. Experimental investigation of FDM-based 3D printed components using multi-criteria decision-making techniques. *J Mech Eng Adv*. 2026;2(3):1-5.

doi: 10.65525/jmea.v2i3.27

35. Parisi M, Di Bella G. Multi-criteria selection of FFF-printed gyroid sandwich structures in PLA and PLA-flax using AHP-TOPSIS. *Machines*. 2026;14(2):162.

doi: 10.3390/machines14020162